Supporting Information for

A Highly Fluorescent Chemosensor for Zn^{2+} and the Recognition Research on Distinguishing Zn^{2+} from Cd^{2+}

Pengxuan Li, [a] *Xiaoyan Zhou,*[a] *Ruoying Huang,*[b] *Lizi Yang,* [a] *Xiaoliang Tang,* [a] *Wei Dou,* [a] *Qianqian Zhao,*[a] *and Weisheng Liu* [*a]

[a] Key Laboratory of Nonferrous Metals Chemistry and Resources Utilization of Gansu Province, State Key Laboratory of Applied Organic Chemistry, College of Chemistry and Chemical Engineering, Lanzhou University, Lanzhou 730000, China

[b] West China School of Public Health Sichuan University, Chengdu 610041, China

Table of contents

8. The effect of pH on L and Cd^{2+}-L at room temperature in HEPES buffer solutions (Fig.S11)

9. Crystal Data and Details of the Structure Determination for $ZnL(NO_3)_2(H_2O)$ and $CdL_2(NO_3)_2$. (Table.S1)

10. Selected Bond Lengths (Å) and Bond Angles (deg) for $ZnL(NO_3)_2(H_2O)$ and $CdL_2(NO_3)_2$. (Table.S2)

11. ^1H-^1H COSY spectra of L, L-Zn^{2+} and L-Cd^{2+} in CD_3CN. (Fig.S12-Fig.S14)

12. ^1H NMR, ^{13}C NMR, ESI-MS and HRMS spectra of L in $CDCl_3$. (Fig. S15-S18)

13. FTIR spectra of L, L-Zn^{2+} and L-Cd^{2+}. (Fig.S19-S21)

1. Absorption titration of L with Zn^{2+} and the association constant of L-Zn^{2+} system in 1:1 CH_3CN/H_2O.

The total binding constant of L with $Zn^{2+}$and Cu^{2+} were studied by the following equations based on a 1:1 complex expression:[1,2]

$$\log\frac{R-R_{min}}{R_{max}-R} = \log[M] + B' - \log\xi(\lambda_2) \quad (1)$$

Where R_{min}, R_{max} and R are the absorbances ratios of $A_{363\ nm}/A_{316\ nm}$ in the absence, presence of saturated Zn^{2+}, and addition of a given amount of Zn^{2+} at aconcentration, respectively. B' represents the binding constant. ξ represents the ratio of the fluorescent intensities at the wavelength ξ (316 nm): $A_{min}(316)/A_{max}(316)$. The total binding constant logK' was deduced (Fig.S1, Fig.S3).

$$A = A_0 + \frac{A_{max}-A_0}{2}\left\{\left(1+\frac{[M]}{C_L}+\frac{1}{C_LK}\right) - \sqrt{(1+\frac{[M]}{C_L}+\frac{1}{C_LK})^2 - 4\times\frac{[M]}{C_L}}\right\} \quad (2)$$

A_0 is the absorbance of L at 363 nm without Cu^{2+}, A is the absorbance of L at 363 nm obtained with Cu^{2+}, and A_{max} is the absorbance of L at 363 nm in the presence of

excess amount of Cu^{2+}. The obtained curve is shown in Fig. S5.

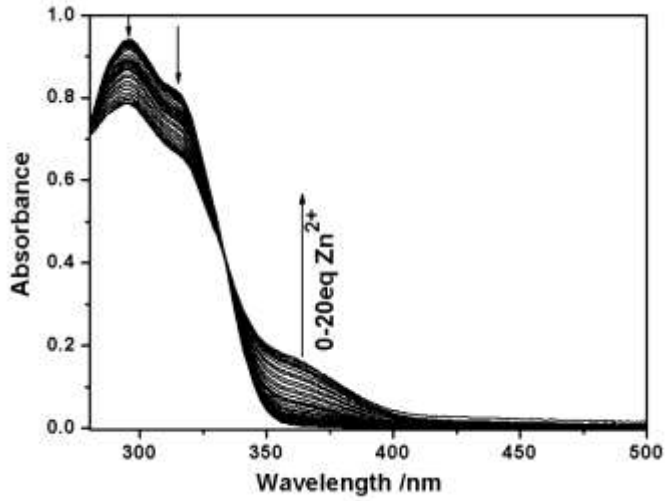

Fig.S1 Absorption spectra of L in HEPES buffer solutions (50 mM, 30 mM NaCl, pH = 7.4, $CH_3CN–H_2O$ = 1:1, v/v) with the increase of $Zn(NO_3)_2$.

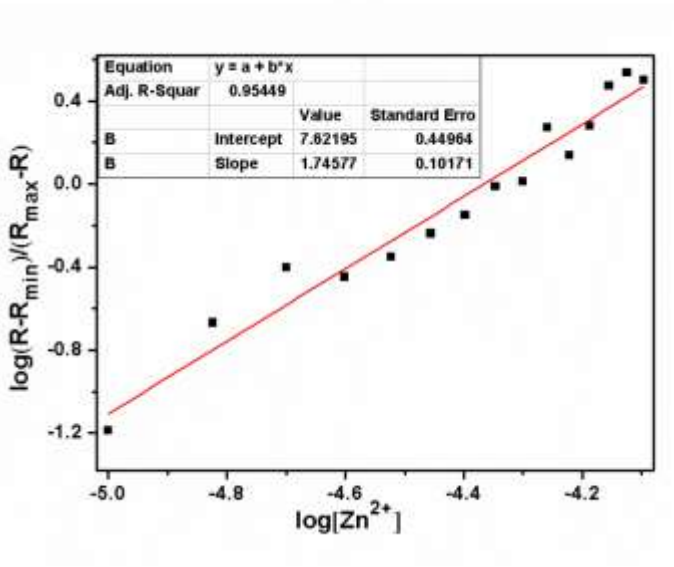

Fig.S2 Ratios between absorbances at 363 nm and at 316 nm (A_{363}/A_{316}) of L in HEPES buffer solutions (50 mM, 30 mM NaCl, pH = 7.4, $CH_3CN–H_2O$ = 1:1, v/v) versus increasing concentration of log[Zn^{2+}]. The concentration of L was 1.0 ×10^{-4} M.

2. Absorption titration of L with Cu^{2+} and the association constant of L-Cu^{2+} system in 1:1 CH_3CN/H_2O.

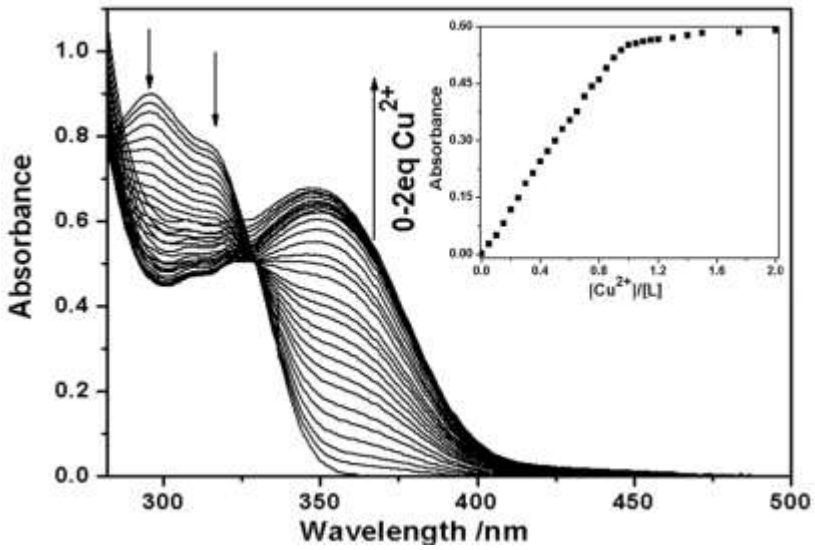

Fig.S3 Absorption spectra of L in HEPES buffer solutions (50 mM, 30 mM NaCl, pH = 7.4, $CH_3CN–H_2O$ = 1:1, v/v) with the increase of Cu $(NO_3)_2$. Inset: The absorbance at 363 nm. [L] = 1.0×10^{-4} M.

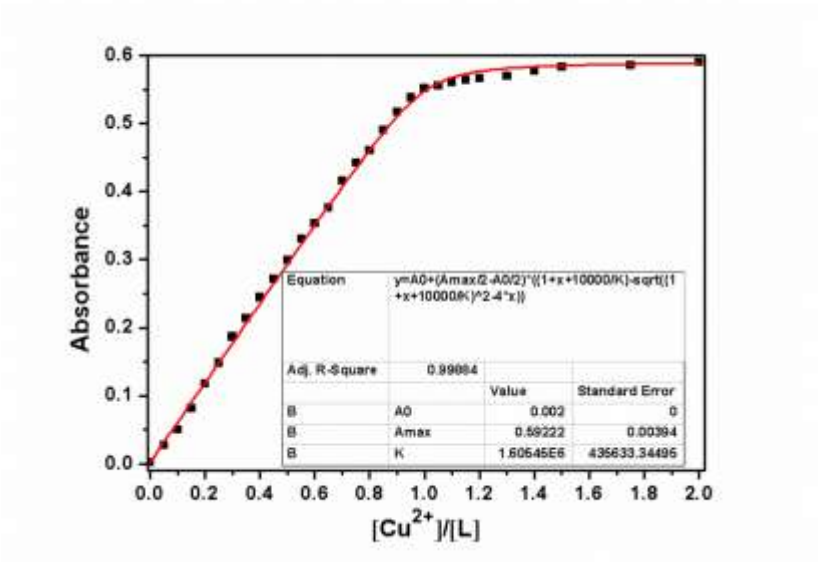

Fig.S4 The absorbance change of L at 363 nm in HEPES buffer solutions (50 mM, 30 mM NaCl, pH = 7.4, $CH_3CN–H_2O$ = 1:1, v/v) with the increase of $Cu(NO_3)_2$. The red line is the nonlinear fitting curve obtained assuming a 1:1 association between L and Cu^{2+}. The association constant was estimated to be 1.6 (± 0.4) × 10^6 M^{-1}. [L] = 1.0×10^{-4} M.

3. Absorption titration of L with Cd^{2+} in acetonitrile.

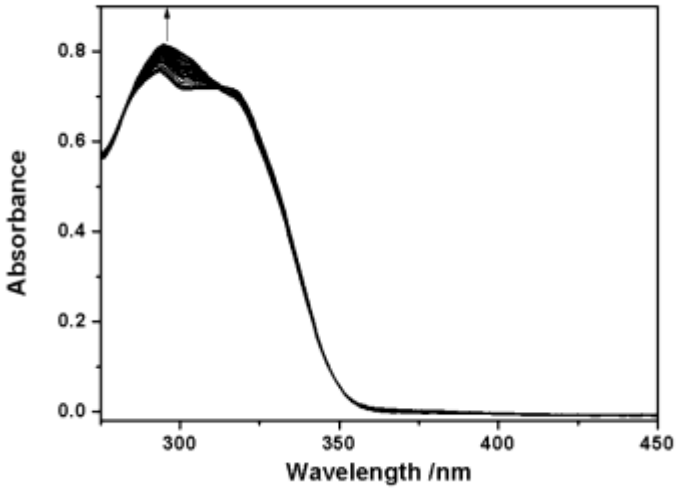

Fig.S5 Absorption spectra of L in acetonitrile with the increase of $Cd(NO_3)_2$. [L] = 1.0 × 10^{-4} M.

4. Absorption titration of L-Cd^{2+} with Cd^{2+} in acetonitrile.

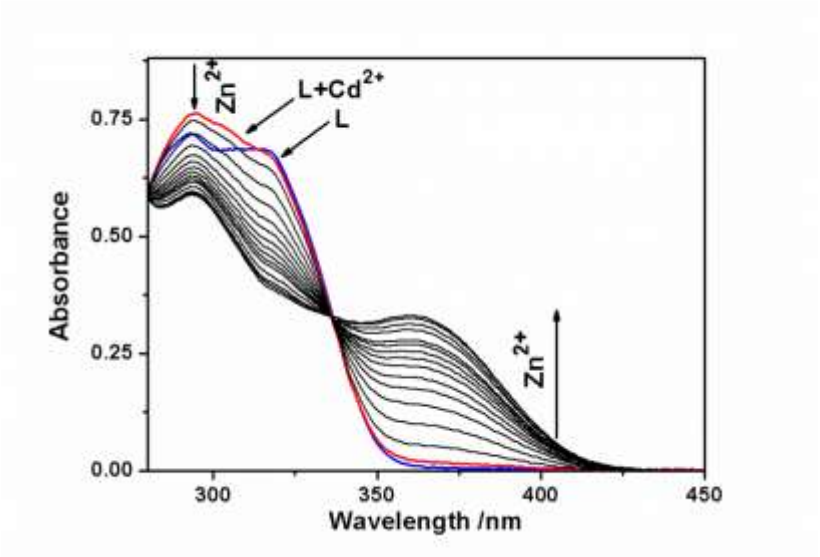

Fig.S6 Absorption spectra of L-Cd^{2+} in acetonitrile with the increase of $Zn(NO_3)_2$.

5. Fluorescence of titration L with Zn^{2+} in acetonitrile.

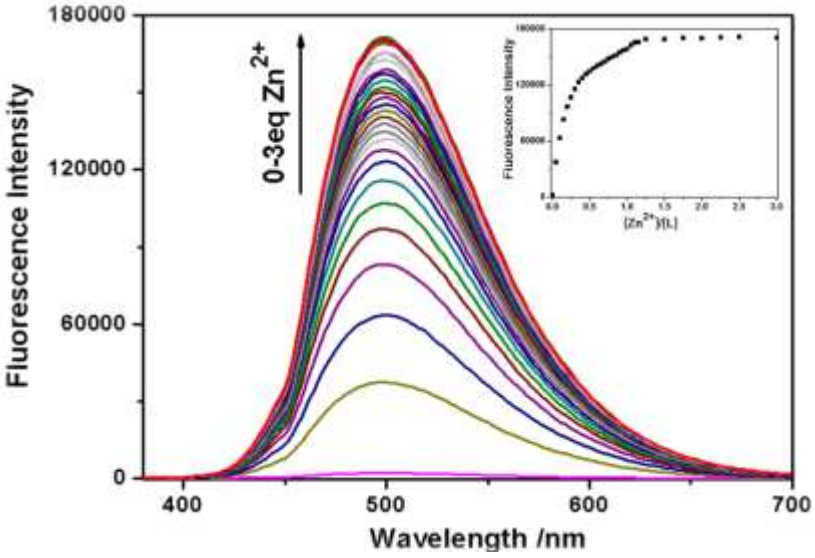

Fig.S7 Fluorescence emission spectra of L upon the addition of $Zn(NO_3)_2$ in acetonitrile. λ_{ex}= 363 nm at room temperature ([L]= 0.10 mM.) (Inset) Corresponding $Zn(NO_3)_2$ titration profile according to the fluorescence intensity, indicating 1:1 stoichiometry for Zn^{2+}/L.

6. Job's plot.

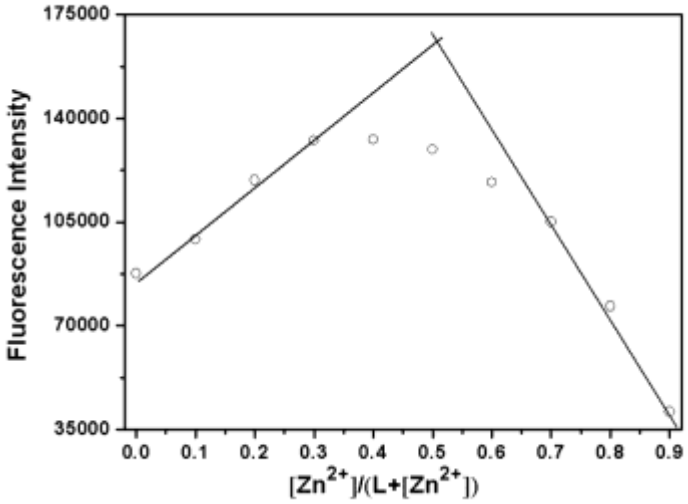

Fig.S8 Job's plot shows the 1:1 binding of L to Zn^{2+}.

7. The detection limit (LOD) and association constant of L-Zn^{2+} in HEPES buffer.

$$F = F_0 + \frac{F_{max}-F_0}{2}\left\{\left(1+\frac{[M]}{C_L}+\frac{1}{C_L K}\right) - \sqrt{\left(1+\frac{[M]}{C_L}+\frac{1}{C_L K}\right)^2 - 4\times\frac{[M]}{C_L}}\right\}$$

F_0 is the absorbance of L at 498 nm without Zn^{2+}, F is the absorbance of L at 498 nm obtained with Zn^{2+}, and F_{max} is the absorbance of L at 498 nm in the presence of excess amount of Zn^{2+}.

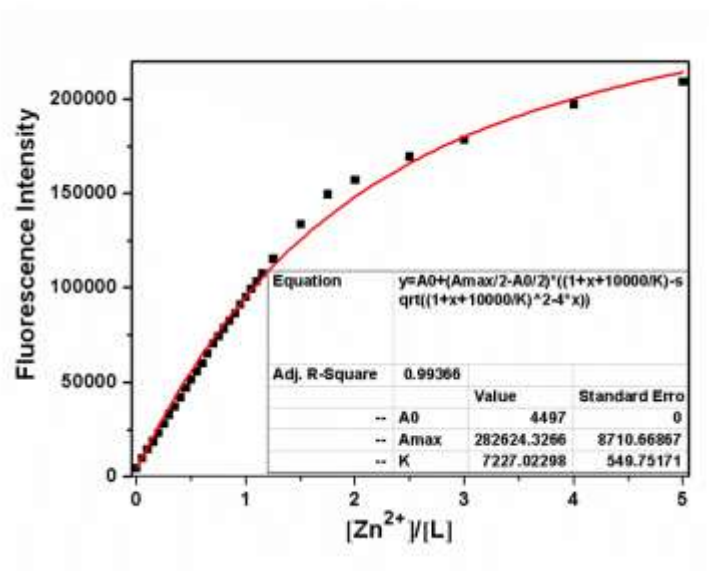

Fig.S9 Change in the fluorescence intensity at 498 nm in HEPES buffer solutions (50 mM, 30 mM NaCl, pH = 7.4, CH_3CN–H_2O = 1:1, v/v) with the increase of $Zn(NO_3)_2$. . The red line is the nonlinear fitting curve obtained assuming a 1:1 association between 1 and Zn^{2+}. The association constant was estimated to be 7.2 (± 0.5) × 10^3 M^{-1}. λ_{ex} = 363 nm, [L] = 1.0 × 10^{-4} M.

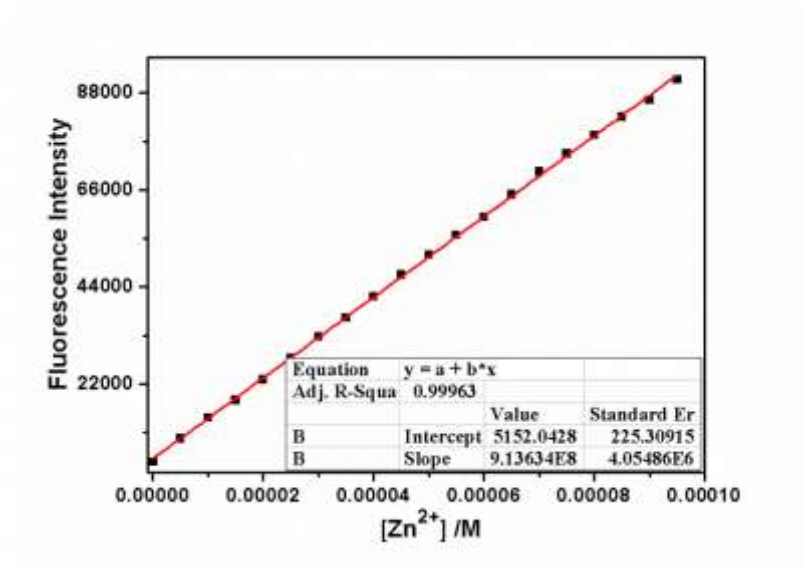

Fig.S10 The linear dynamic response of L for Zn^{2+} and the determination of the detection limit (LOD) for Zn^{2+} in HEPES buffer (50 mM, 30 mM NaCl, pH = 7.4, $CH_3CN–H_2O$ = 1:1, v/v).

8. **The effect of pH on L and Cd^{2+}-L at room temperature in HEPES buffer solutions**

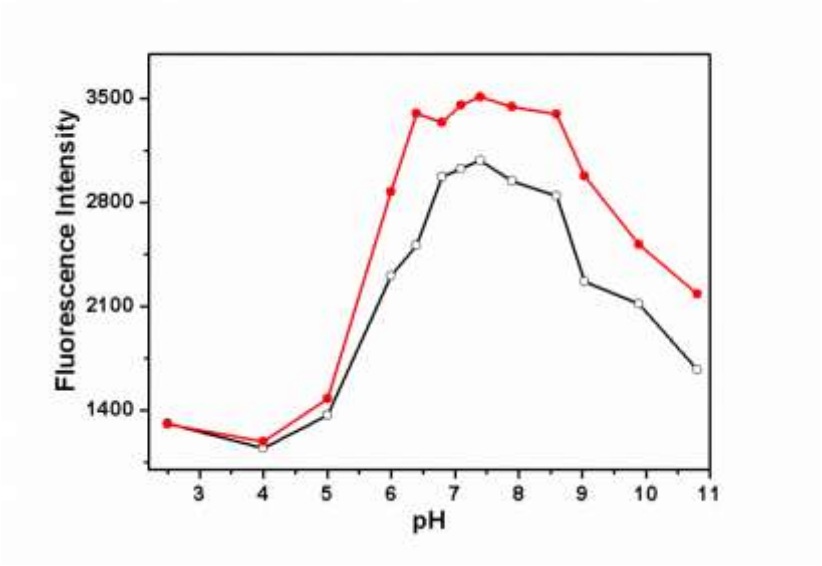

Fig.S11 Fluorescence intensities of L and Cd^{2+}-L at various pH values at room temperature, HEPES buffer solutions (50 mM, 30 mM NaCl, pH = 7.4, $CH_3CN–H_2O$ = 1:1, v/v).

References:

(1) Zhou, X. Y.; Yu, B. R.; Guo, Y. L.; Tang, X. L.; Zhang, H. H.; Liu, W. S. *Inorg. Chem*. **2010**, *49*, 4002.

(2) Zhou, J. A.; Tang, X. L.; Cheng, J.; Ju, Z. H.; Yang, L. Z.; Liu, W. S.; Chen, C. Y. and Bai, D. C. *Dalton Trans*. **2012**, *41*, 10626.

9. Crystal Data and Details of the Structure Determination for $Zn(L)(NO_3)_2(H_2O)$ and $Cd(L)_2(NO_3)_2$.

Table S1. Crystal Data and Details of the Structure Determination for $Zn(L)(NO_3)_2(H_2O)$ and $Cd(L)_2(NO_3)_2$

	$Zn(L)(NO_3)_2(H_2O)$	$Cd(L)_2(NO_3)_2$
Empirical formula	$C_{24}H_{22}N_6O_{10}Zn$	$C_{48}H_{40}N_{10}O_{12}Cd$
Temperature /K	296(2)	293 (2)
Formula weight	619.85	984.12
Crystal system	Monoclinic	Triclinic
Space group	$P2_1/c$	$P\bar{1}$
a/Å	7.687 (4)	10.4777 (5)
b/Å	20.840 (11)	10.5164 (5)
c/Å	16.689 (7)	11.2131 (5)
α /deg	90	87.605 (2)
β /deg	107.626 (19)	88.003 (2)
γ /deg	90	83.719 (2)
V/Å^3	2548 (2)	1226.49 (10)
Z	4	1
Dcalcd /kg m^{-3}	1.616	1.480
μ/mm^{-1}	1.035	0.521
F(000)	1272	560
Independent reflections (Rint)	0.0614	0.0098
Reflns collectes /unique	18160/ 4748	6278 / 4316
Data/restraints /params	4748/0/ 374	4316 / 0 / 342
goodness-of-fit on F^2	1.003	1.031
final R indices [I > 2σ (I)]	R_1 = 0.0560 wR_2 = 0. 1261	R_1 = 0.0337 wR_2 = 0.1107
R indices (all data)	R_1= 0.0987 wR_2= 0.1435	R_1 = 0.0363 wR_2 =0.1142
Residual electron density/e Å^{-3}	-0.444 to 0.906	-0.251 to 0.876

10. Selected Bond Lengths (Å) and Bond Angles (deg) for $Zn(L)(NO_3)_2(H_2O)$ and $Cd(L)_2(NO_3)_2$.

Table S2. Selected Bond Lengths (Å) and Bond Angles (deg)

$Zn(L)(NO_3)_2(H_2O)$		$Cd(L)_2(NO_3)_2$	
Zn1—O3	1.978 (3)	Cd1—O1	2.301 (2)
Zn1—O7	2.046 (4)	Cd1—O1^{i}	2.301 (2)
Zn1—O10	2.127 (4)	Cd1—N1^{i}	2.314 (2)
Zn1—N3	2.151 (4)	Cd1—N1	2.314 (2)
Zn1—O4	2.207 (4)	Cd1—O4	2.346 (3)
Zn1—O5	2.229 (4)	Cd1—O4^{i}	2.346(3)
O3—Zn1—O7	110.66 (13)	O1—Cd1—O1^{i}	180.00 (11)
O3—Zn1—O10	88.60 (14)	O1—Cd1—N1^{i}	91.87 (8)
O7—Zn1—O10	84.06 (17)	O1^{i}—Cd1—N1^{i}	88.13 (8)
O3—Zn1—N3	97.46 (13)	O1—Cd1—N1	88.13 (8)
O7—Zn1—N3	96.50 (14)	O1^{i}—Cd1—N1	91.87 (8)
O10—Zn1—N3	173.26 (15)	N1^{i}—Cd1—N1	180.0
O3—Zn1—O4	99.43 (13)	O1—Cd1—O4	88.49 (9)
O7—Zn1—O4	147.07 (14)	O1^{i}—Cd1—O4	91.51 (9)
O10—Zn1—O4	83.60 (16)	N1^{i}—Cd1—O4	98.42 (9)
N3—Zn1—O4	92.44 (14)	N1—Cd1—O4	81.58(9)
O3—Zn1—O5	156.78 (14)	O1—Cd1—O4^{i}	91.51 (9)
O7—Zn1—O5	91.49 (14)	O1^{i}—Cd1—O4^{i}	88.49 (9)
O10—Zn1—O5	86.80 (14)	N1^{i}—Cd1—O4^{i}	81.58 (9)
N3—Zn1—O5	86.48 (13)	N1—Cd1—O4^{i}	98.42(9)
O4—Zn1—O5	57.44 (14)	O4—Cd1—O4^{i}	180.00 (14)

11. ^{1}H-^{1}H COSY spectra of L, L-Zn^{2+} and L-Cd^{2+} in CD_3CN.

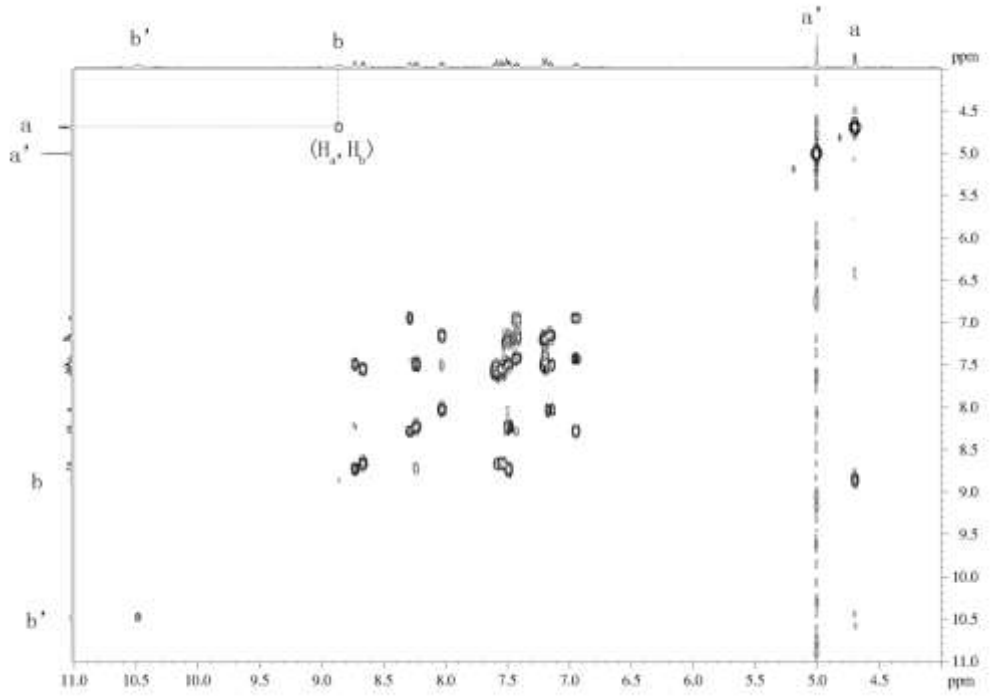

Fig. S12 ^{1}H-^{1}H COSY spectra of L in CD_3CN.

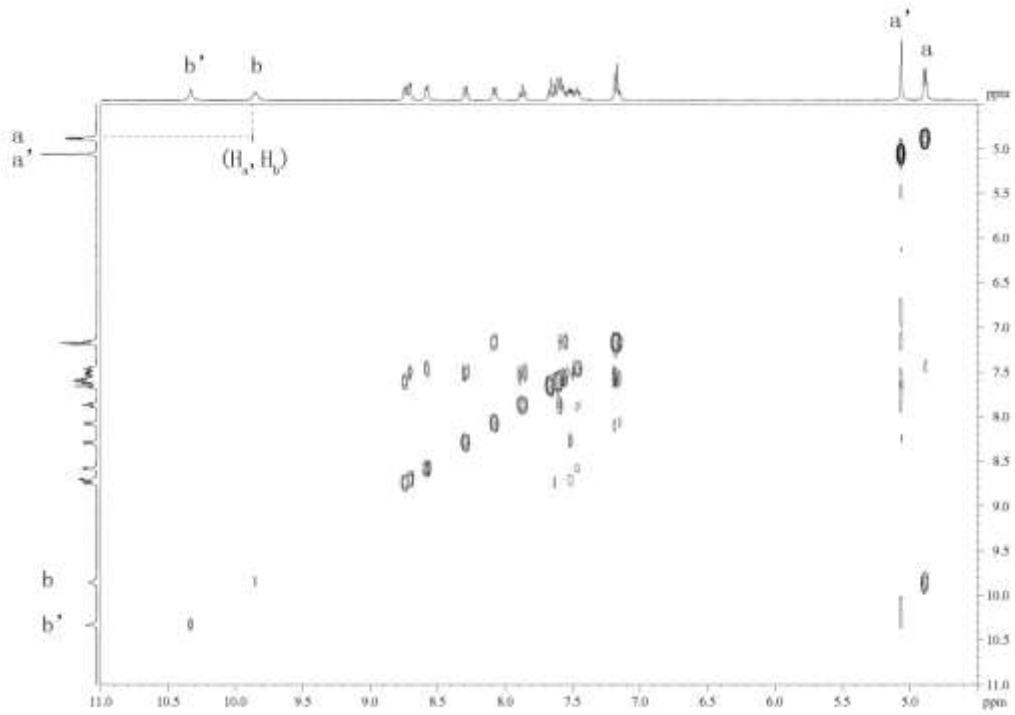

Fig. S13 ^{1}H-^{1}H COSY spectra of L-Cd^{2+} in CD_3CN.

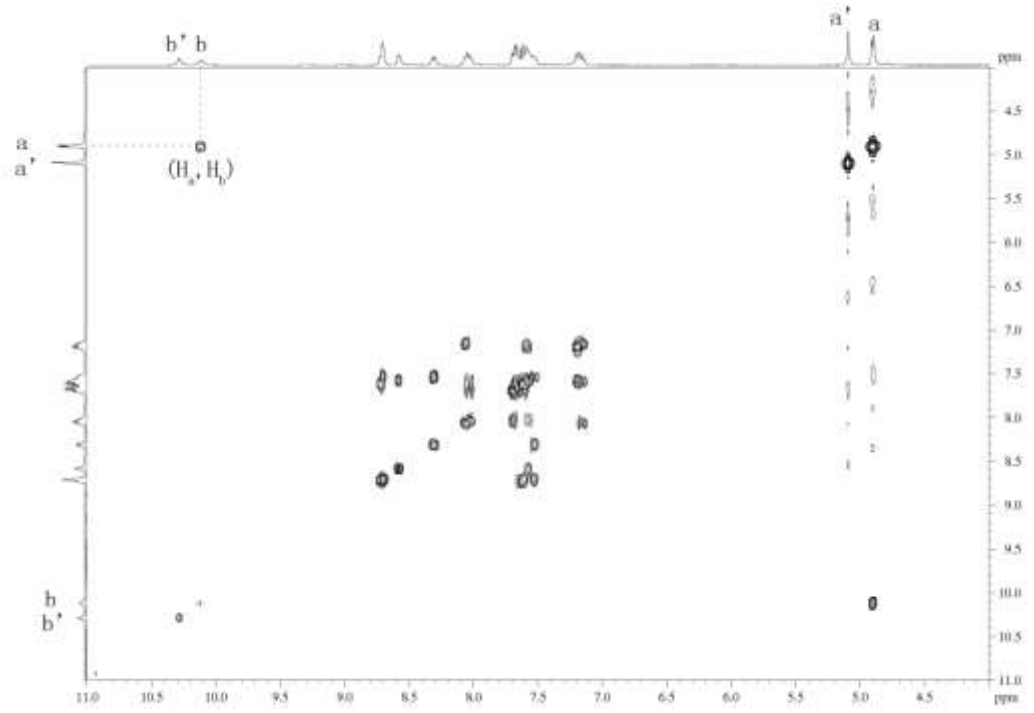

Fig. S14 ^{1}H-^{1}H COSY spectra of L-Zn^{2+} in CD_3CN.

12. ^{1}H NMR, ^{13}C NMR ,ESI-MS and HRMS spectra of L in $CDCl_3$.

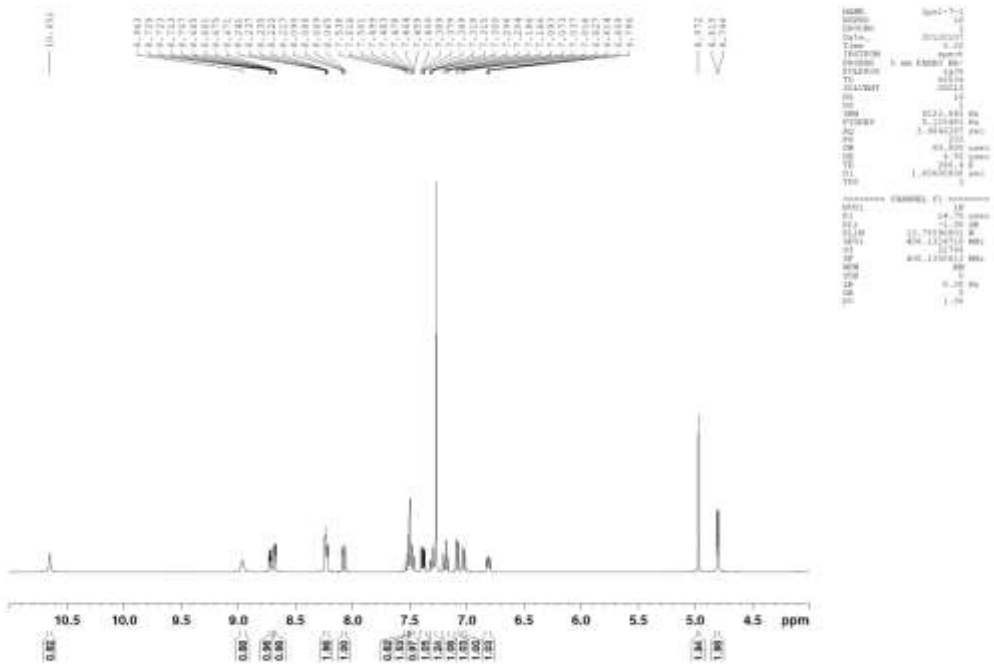

Fig.S15 ^{1}H NMR spectra of L in $CDCl_3$

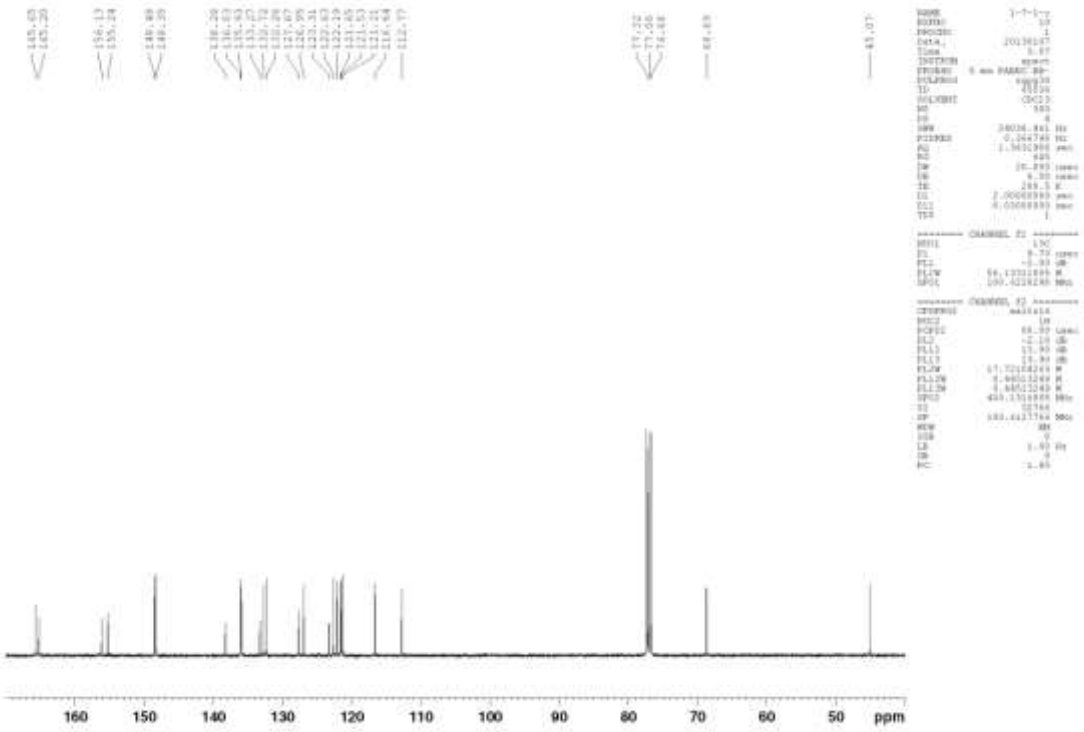

Fig.S16 ^{13}C NMR spectra of L in $CDCl_3$

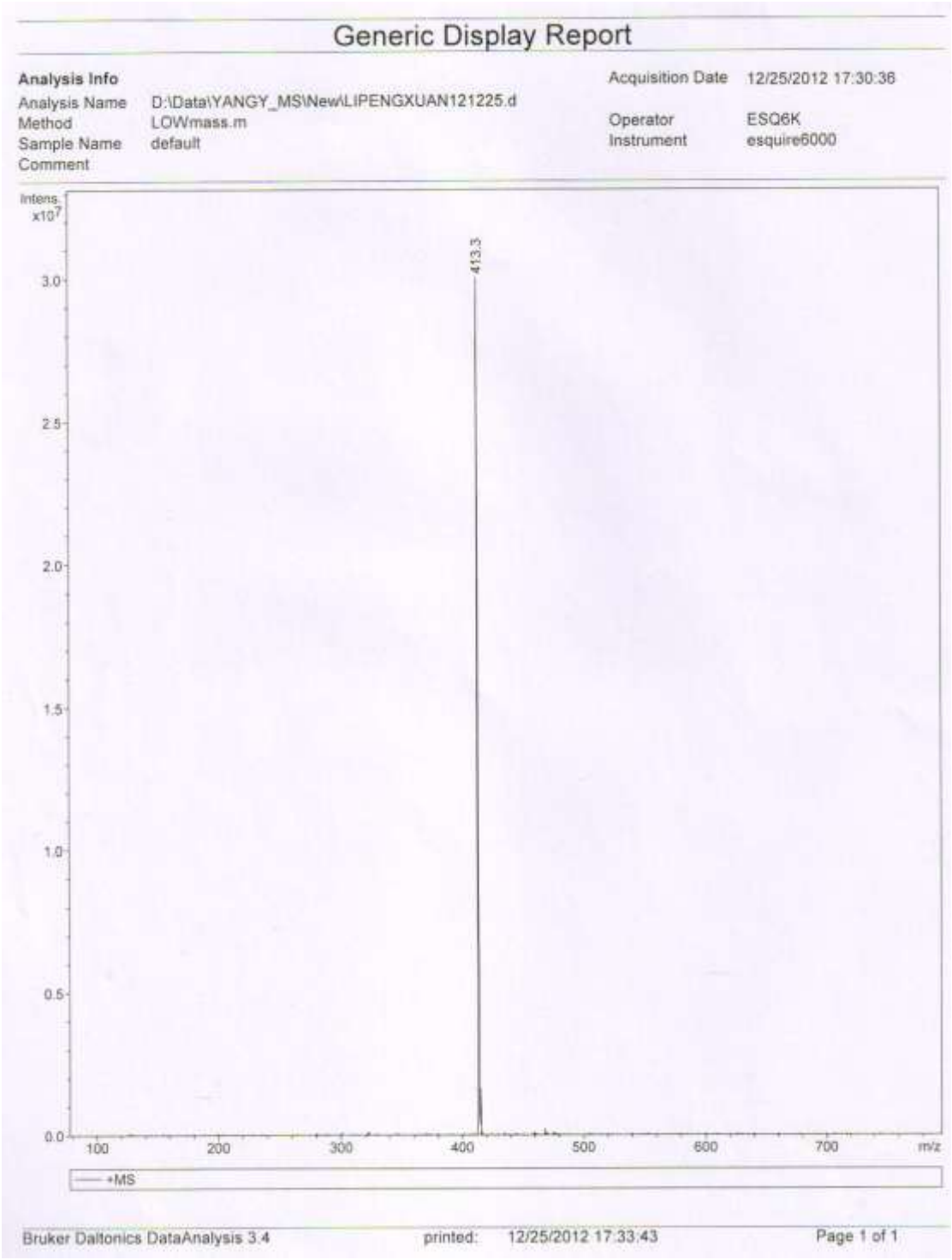

Fig.S17 ESI-MS spectra of L

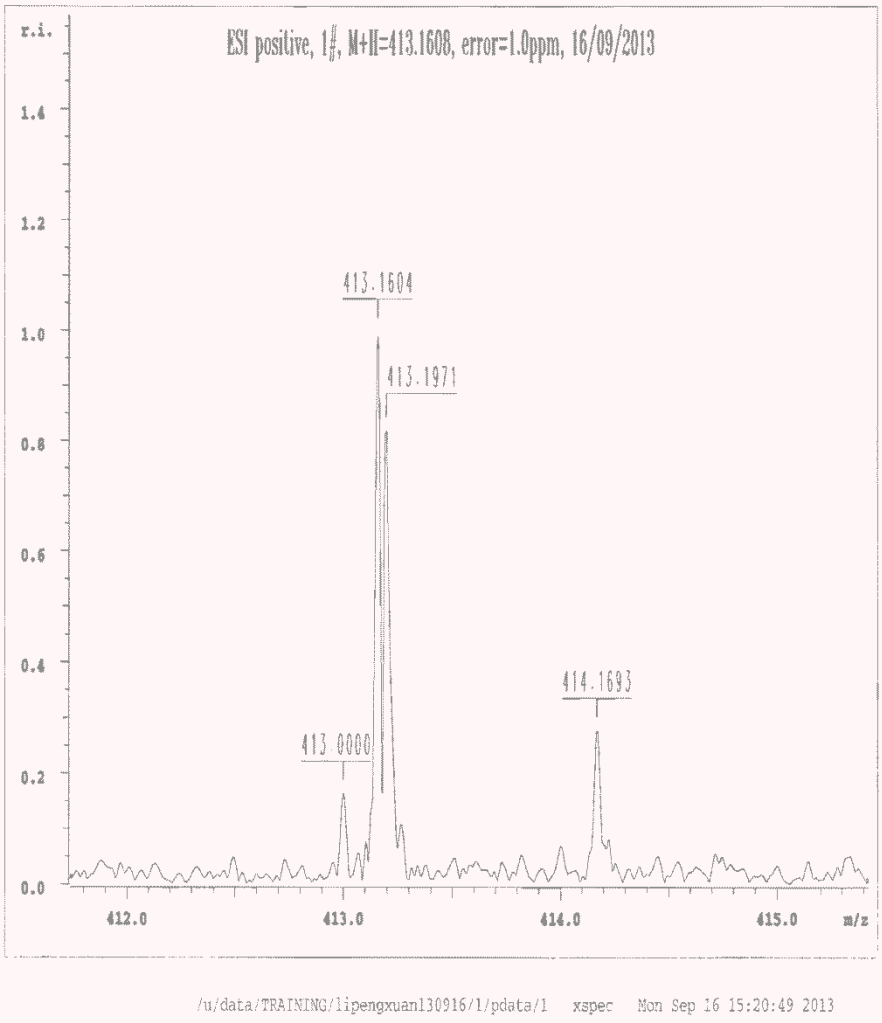

Fig.S18 HRMS spectra of L

13. FTIR spectra of L, L-Zn^{2+} and L-Cd^{2+}.

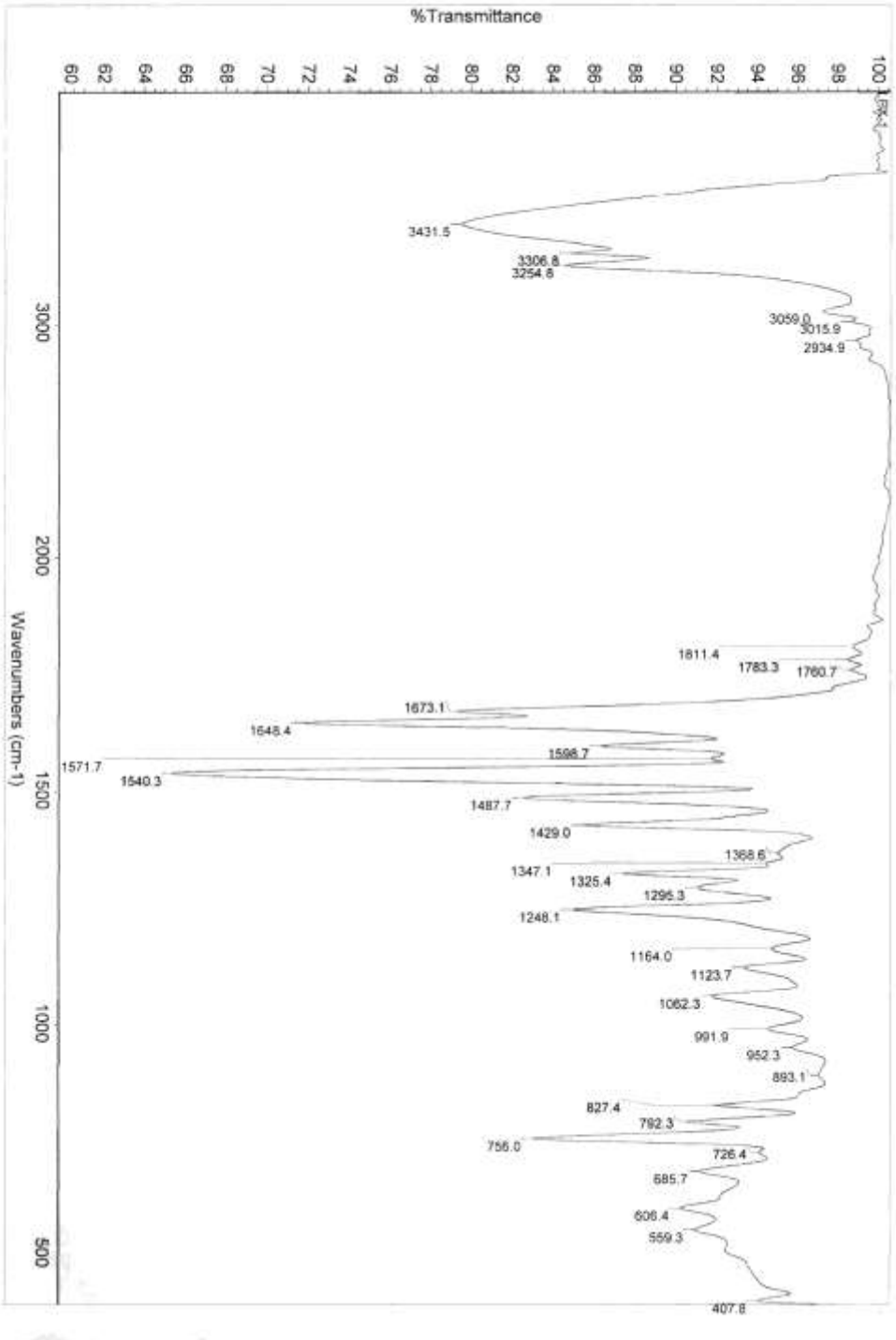

Fig.S19 FTIR spectra of L

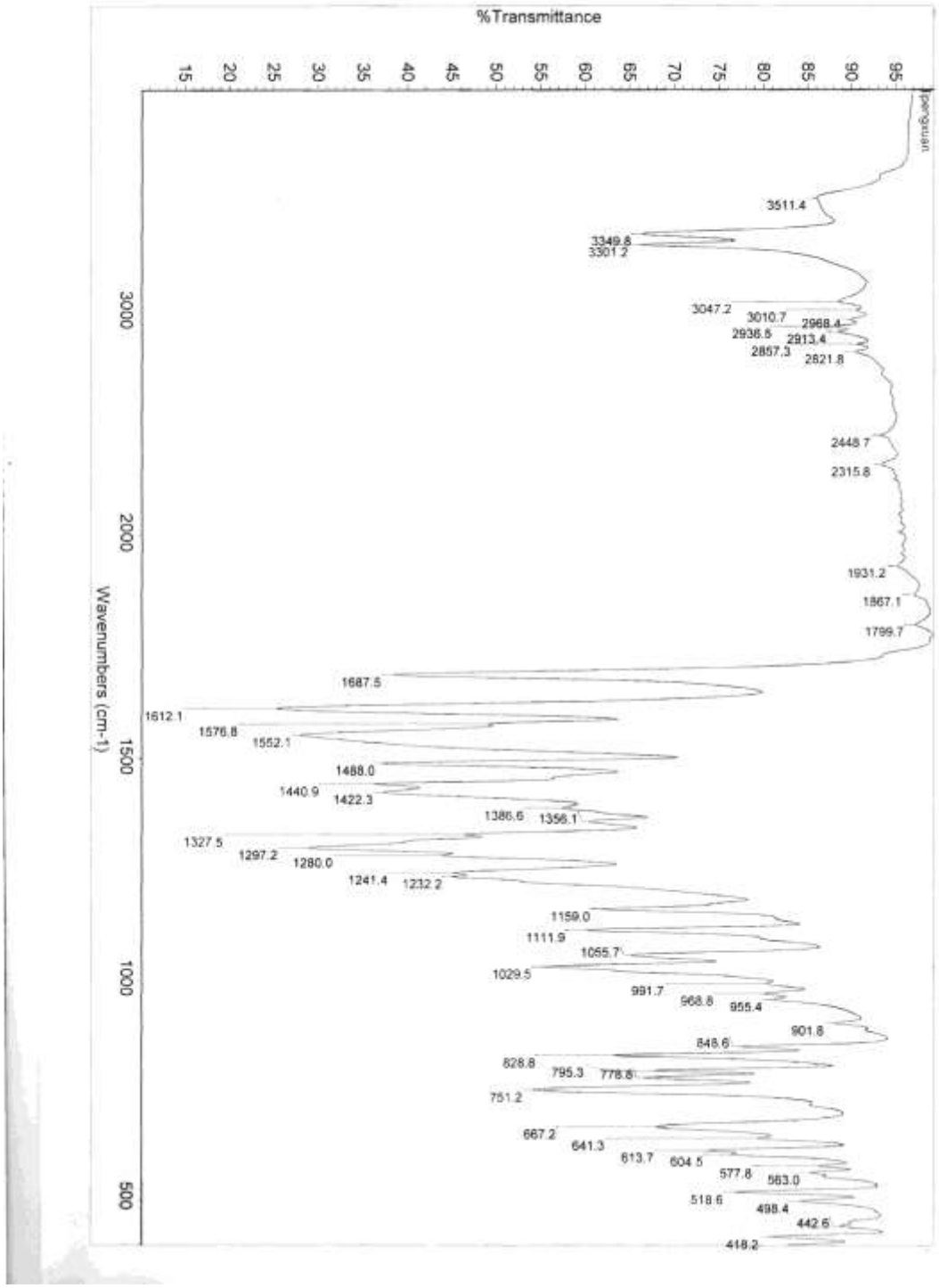

Fig.S20 FTIR spectra of L-Cd^{2+}

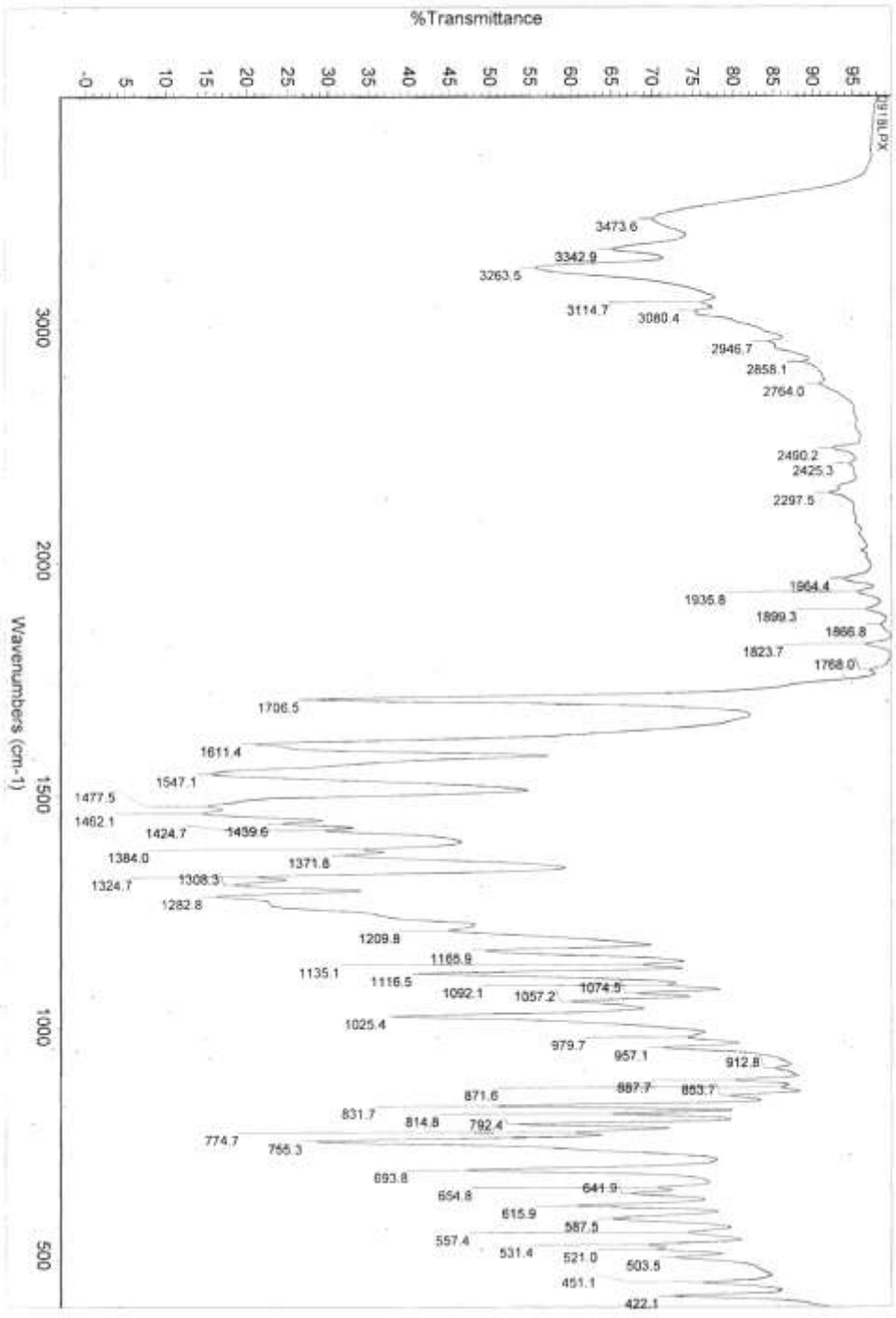

Fig.S21 FTIR spectra of L-Zn^{2+}